*Global Journal of Mathematical Sciences Vol2-1* (2013) 20–32

# DNS Study for the Origin of the Chaos in Late Boundary Layer Transition

**ABSTRACT:** This paper is devoted to the investigation of the origin and mechanism of chaos in late boundary layer transition over a flat plate without pressure gradient. The chaotic flow not only exists at the last stage of flow transition but also in turbulence flow. According to existing theory, the formation of such kind of chaos was considered due to big background noise and non-periodic boundary condition in spanwise direction. It was assumed that the large ring structure is first affected by background noises and then the change of large ring structure affects the small length scale quickly, which directly leads to chaos and finally formation of turbulence. However, by careful analysis of our high order DNS results, we believe that the internal instability of multiple ring cycles structure triggered by overlapping of these cycles is the main reason.Furthermore, A significant asymmetric phenomenon is originated from the second cycle in middle of both streamwise and spanwise direction when third cycle overlaps first and second cycles. The chaotic phenomenon spreads to the top level through an important process known as "ejections" which carries low speed fluid from bottom to top. Eventually,the whole flow domain becomes asymmetric and chaotic.

## Nomenclature

$M_\infty$=Mach number
Re= Reynolds number
$\delta_{in}$=inflow displacement thickness
$T_w$=wall temperature
$T_\infty$=free stream temperature
$Lz_{in}$= height at inflow boundary
$Lz_{out}$= height at outflow boundary
$Lx$= length of computational domain along x direction
$Ly$= length of computational domain along y direction
$Lz$= length of computational domain along x direction
$x_{in}$=distance between leading edge of flat plate and upstream boudnary of computational domain
$A_{2d}$=amplide of 2D inlet disturbance
$A_{3d}$=amplide of 3D inlet disturbance
$\omega$=frequency of inlet disturbance
$\alpha_{2d}, \alpha_{3d}$=two and three dimensional streamwise wave number of inlet disturbance
$\beta$=spanwise wave number of inlet disturbance
R=ideal gas constant
$\rho$=ratio of specfic heats
$\mu_\infty$= viscosity

## 1 Introduction

Turbulence, one of the top secrets of the nature, in general, is composed of two parts: small length scale generation and chaos formation. Although the turbulence origination and formation in late boundary layer transition has become a subject of intense reserach for over a century[4-5,10,13,15-16,21 etc.], there are only a few research papers about the origin of chaotic flow formation. One main reason may be that fluid dynamic community always relied on the classical theory at least for turbulence generation and sustenance. According to the classical theory [18,19 etc.],the turbulence is generated when the large vortices in late stage of boundary layer transition break down into small vortices (small eddies). Unfortunately, the vortex breakdown and reconnection process couldn't be observed by our DNS [20].

While taking into account earlier research work about flow chaos, one of the milestone works was done by Daniel Meyer and his colleagues [1-2]. They believed that "the inclined high-shear layer between the legs of the vortex exhibits increasing phase jitter (i.e. chaotic flow) starting from its tip towards the wall region". However, from our high order numerical simulation, we observed a phenomenon [3,23] which is completely different from the theory given by Meyer and his co-workers. We use periodic boundary condition in spanwise direction and disturbances are present only at inflow, outflow and far field. Still, we observe chaotic flow. So, it is unlikely to happen flow chaos due to back ground noise or by the use of non periodic condition in spanwise direction.

The understanding of turbulent flow in moving fulid is one of the most intriguing and frustrating - still fascinting -flow in morden classical physics. It is not very clear how or why turbulence occurs nor it's behavior can be predicted with any degree of accuracy, even in very simple flow. There isn't any precise definition of turbulence flow, but it can be expected to exhibit some of distinct features. In general, turbulence flow is characterized by chaotic and stochastic property changes in time and space. It also consists of extremely large range of length and time scales, Then obviously some of important questions may come to our mind such as from where random fluctuation starts and by which mechanism flow becomes chaotic? We thoroughly investigate a huge number of data base obtained by our high order DNS and try to trace early

Received ??

location and time step for such kind of chaotic flow. In the section 4,We have presented a hypothesis while trying to reveal new mechanism of formation of such kind messy flow, which still have to be verified analytically and experimentally .

Since, skin friction in turbulent boundary layer is always higher that in laminar boundary layer [22] so the people who are dealing with design of aircraft always willing to delay transition process in boundary layer (reducing skin friction in boundary layer of aircraft means reduction in consumption of fuel). In this context, our present paper may obtain some attention.

A $\lambda_2$ eigenvalue technology developed by Jeong and Hussain [9] is used for visualization of vortex structures formed by interaction of non-linear evolution of T-S wave in the late boundary layer transition.

# 2 Case Setup and Code Validation

## 2.1 Case Setup

The computational domain is displayed in Figure 1. The grid level is $1920 \times 128 \times 241$, representing the number of grids in streamwise (x), spanwise (y), and wall normal (z) directions. The grid is stretched in the normal direction and uniform in the streamwise and spanwise directions. The length of the first grid interval in the normal direction at the entrance is found to be 0.43 in wall units ($Y^+$=0.43). The parallel computation is accomplished through the Message Passing Interface (MPI) together with domain decomposition in the streamwise direction (Figure 2). The flow parameters, including Mach number, Reynolds number, etc are listed in Table 1. Here, $x_{in}$ represents the distance between leading edge and inlet,Lx ,Ly ,$Lz_{in}$ are the lengths of the computational domain in x-, y-, and z-directions, respectively, and $T_w$ is the wall temperature.

Table 1: Flow parameters

| $M_\infty$ | $Re$ | $x_{in}$ | $Lx$ | $Ly$ | $Lz_{in}$ | $T_w$ | $T_\infty$ |
|---|---|---|---|---|---|---|---|
| 0.5 | 1000 | $300.79\delta_{in}$ | $798.03\delta_{in}$ | $22\delta_{in}$ | $40\delta_{in}$ | 273.15K | 273.15K |

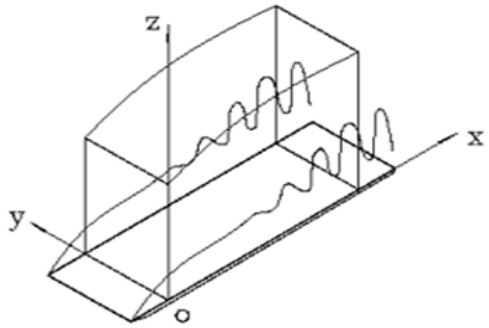


Figure 1: Computation domain.

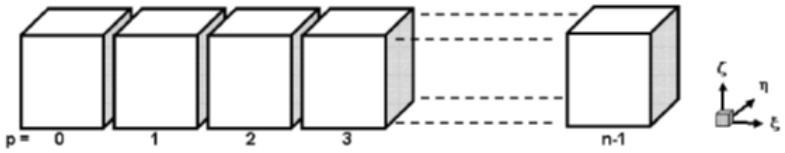


Figure 2: Domain decomposition along the streamwise direction in the computational space

## 2.2 Code Validation

The DNS code "DNSUTA" has been validated by NASA Langley and UTA researchers [11-12,14] carefully to make sure the DNS results are correct.

### 2.2.1 Comparison with Linear Theory

Figure 3 compares the velocity profile of the T-S wave given by our DNS results to linear theory. Figure 4 is a comparison of the perturbation amplification rate between DNS and LST. The agreement between linear theory and our numerical results is quite good.

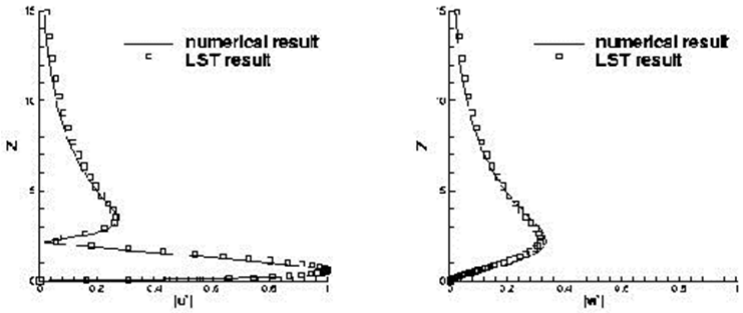


Figure 3: Comparison of the numerical and LST velocity profiles at $Re_x = 394300$

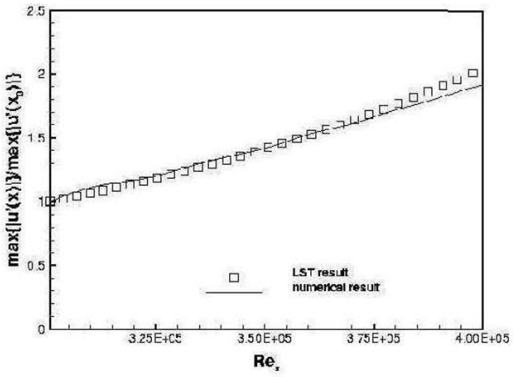


Figure 4: Comparison of the perturbation amplification rate between DNS and LST

### 2.2.2 Grid Convergence

The skin friction coefficient calculated from the time-averaged and spanwise-averaged profile on a coarse and fine grid is displayed in Figure 5. The spatial evolution of skin friction coefficients of laminar flow is also plotted out for comparison. It is observed from these figures that the sharp growth of the skin-friction coefficient occurs after $x \approx 450\delta_{in}$,which is defined as the "onset point". The skin friction coefficient after transition is in good agreement with the flat-plate theory of turbulent boundary layer by Cousteix in 1989 (Ducros, 1996)[12]. Figures 5(a) and 5(b) also show that we get grid convergence in skin friction coefficients.

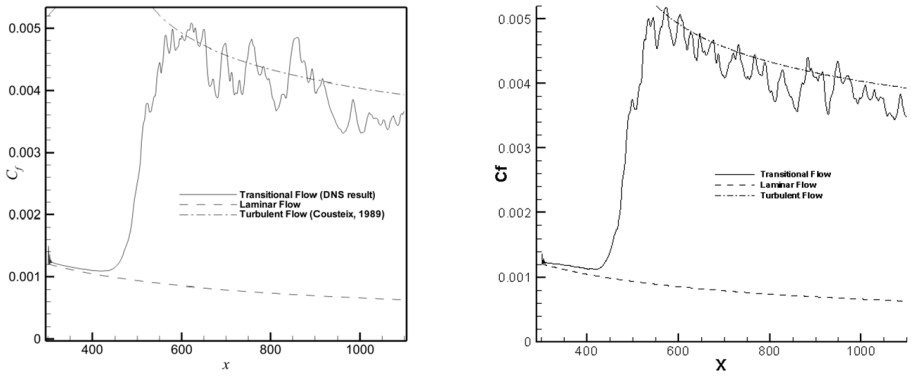


(a) Coarse grids (960×64 × 121) (b) Fine grid (1920×128 × 241)

Figure 5: Streamwise evolutions of the time-and spanwise-averaged skin-friction coefficient

### 2.2.3 Comparison with Log Law

Time-averaged and spanwise-averaged streamwise velocity profiles for various streamwise locations in two different grid levels are shown in Figure 6. The inflow velocity profiles at x=300.79$\delta_{in}$ is a typical laminar flow velocity profile. At x=632.33$\delta_{in}$ ,the mean velocity profile approaches a turbulent flow velocity profile (Log law). This comparison shows

that the velocity profile from the DNS results is turbulent flow velocity profile and the grid convergence has been realized.

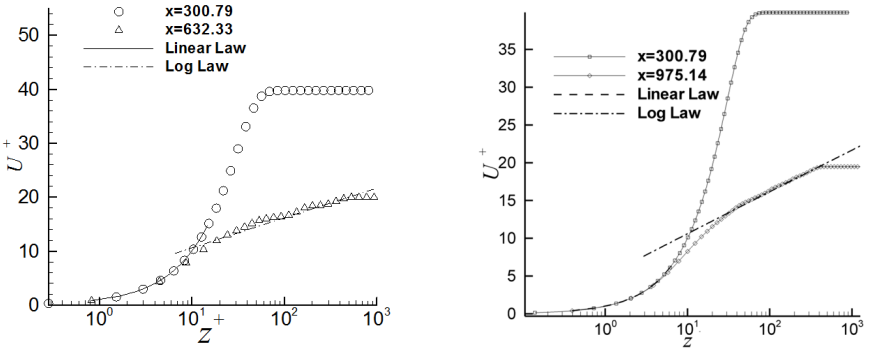


(a) Coarse grids (960×64 × 121) (b) Fine grid (1920×128 × 241)

Figure 6: Log-linear plots of the time-and spanwise-averaged velocity profile in wall unit

## 2.3 Spectra and Reynolds Stress (Velocity) Statistics

Figure 7 shows the spectra in x- and y- directions. The spectra are normalized by z at location of $Re_x = 1.07 \times 10^6$ and $y^+ = 100.25$ . In general, the turbulent region is approximately defined by $y^+ > 100$ and $y/\delta < 0.15$ . In our case, The location of $y/\delta = 0.15$ for $Re_x = 1.07 \times 10^6$ is corresponding to $y^+ \approx 350$ , so the points at $y^+ = 100$ and 250 should be in the turbulent region. A straight line with slope of -3/5 is also shown for comparison. The spectra tend to tangent to the $\kappa^{-3/5}$ law. The large oscillations of the spectra can be attributed to the inadequate samples in time when the average is computed.

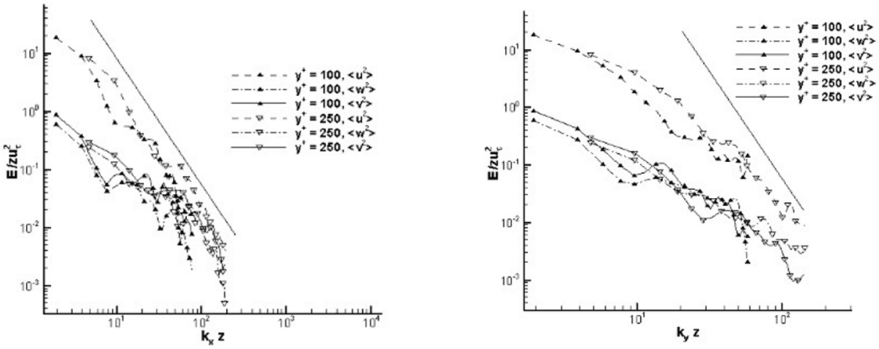


(a) Spectra in x direction (b) Spectra in y direction

Figure 7: Spectral analysis

### 2.3.1 Comparison with Other DNS

Although we cannot compare our DNS results with those given by Borodulin et al [4] quantitatively, we still can find that the shear layer structures are very similar in two DNS computations in Figure 8.

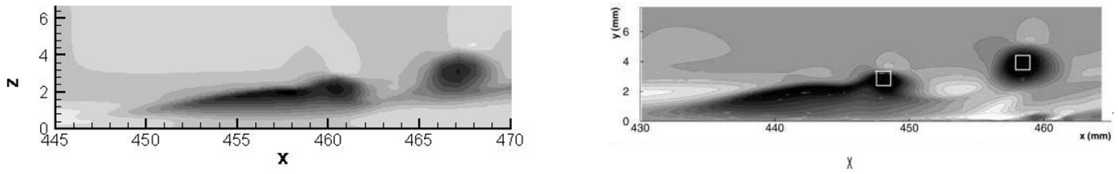


(a) Our DNS (b) Borodulin et al (2002)

Figure 8: Qualitatively comparison of contours of streamwise velocity disturbance u in the (x, z)-plane (Light shades of gray correspond to high values)

### 2.3.2 U-shaped Vortex in Comparison with Experimental Results

Figure 9(a) (Guo et al,[8]) represents an experimental investigation of the vortex structure including ring-like vortex and barrel-shaped head (U-shaped vortex). The vortex structures of the nonlinear evolution of T-S waves in the transition process are given by DNS in Figure 9(b). By careful comparison between the experimental work and DNS, we note that the experiment and DNS agree with each other in a detailed flow structure comparison. This cannot be obtained by accident, but provides the following clues:

1. Both DNS and experiment are correct.
2. Disregarding the differences in inflow boundary conditions (random noises VS enforced T-S waves) and spanwise boundary conditions (non-periodic VS periodic) between experiment and DNS, the vortex structures are same.
3. No matter K-, H- or other types of transition, the final vortex structures are same.
4. There is an universal structure for late boundary layer transition.
5. Turbulence has certain coherent structures (CS) for generation and sustenance.

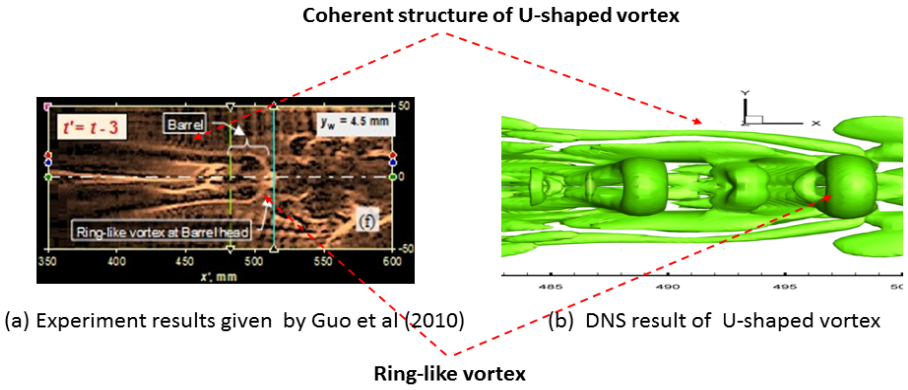


Figure 9: Qualitative vortex structure comparison with experiment

**All these verifications and validations above show that our code is correct and our DNS results are reliable.**

# 3 Our DNS Observations on "Chaotic Flow"

## 3.1 Nature of Coherent Structure in Late Stage of Transition

To gain additional insight for the flow chaos process in very late stage of the transition, here we present a short review of development and evolution of coherent vertical structures which are produced by interaction of non linear Tollmien-Schlichting (T-S) wave in the late stage. Blasius solution with enforced disturbunce is introduced into inlet as a laminar base inflow . The disturbance includes a two-dimensional T-S wave and a pair of conjugate three-dimensional T-S waves. The inflow has a form:
$q = q_{lam} + A_{2d}q'_{2d}e^{i(\alpha_{2d}x-\omega t)} + A_{3d}q'_{3d}e^{i(\alpha_{3d}x\pm\beta y-\omega t)}$
where $q = [u, v, w, T]^t$ ,$q_{lam}$ is the Blasius solution for a two-dimensional laminar flat-plate boundary layer. $e^{i(\alpha_{2d}x-\omega t)}$ and $e^{i(\alpha_{3d}x\pm\beta y-\omega t)}$ are 2-D and 3-D pertubation waves (T-S wave). For identification purpose, we use $\lambda_2$-eigenvalue technology developed by Jeong and Hussain [9]. Figure 10 is the evolution of time dependent vortical structure at the stage of transition. Actually, the late stage of transition starts with development of two pairs of counter-rotating $\Lambda$(horse shoe)-vortices at time t=6T (figure 10(a)). These structures are rather short at the beginning (x=412-420 $\delta_{in}$). They are continuously stretching during the evolution- velocity is different at differnt parts of the structures- and become much larger while moving downstream. While moving downstream furthermore, the vortex tips and $\Omega$-(hairpin) vortices appear. Perfectly circular and perpendicular ring like vortices are generated by the interaction of primary and secondary streamwise vortices and they are gradually lifted up due to boundary layer mean velocity profile [4-6]. Two important phenomena in late stage, namely "sweep" and "ejection"[8] are connected with ring like vortices. The sweep motion between legs of ring like vortices brings low speed flow from boundary layer bottom to high speed zone near the inviscid area. So, high shear layer is formed just above the ring legs. This shear layer is very unstable and multiple rings are formed by following first Helmholtz vortex conservation law (Figure 10(b)). For detail mechanism [4-8,13]. From Figure 10(c), we observe that second ring cycle overlaps first cycle (x= 472 - 490$\delta_{in}$). This phenomenon will be described in more detail in section (3.3). The coherent vertical structures which were demonstrating very salient feature at the beginning of late stage, now started to entangle each other. As we see from Figure 10(d), the third level cycle just starts to overlap previous cycles in time step t=10.3T at $x \approx 500$. The complicated and nonlinear flow field in late stage of time can be visualizing from Figure 10(e).

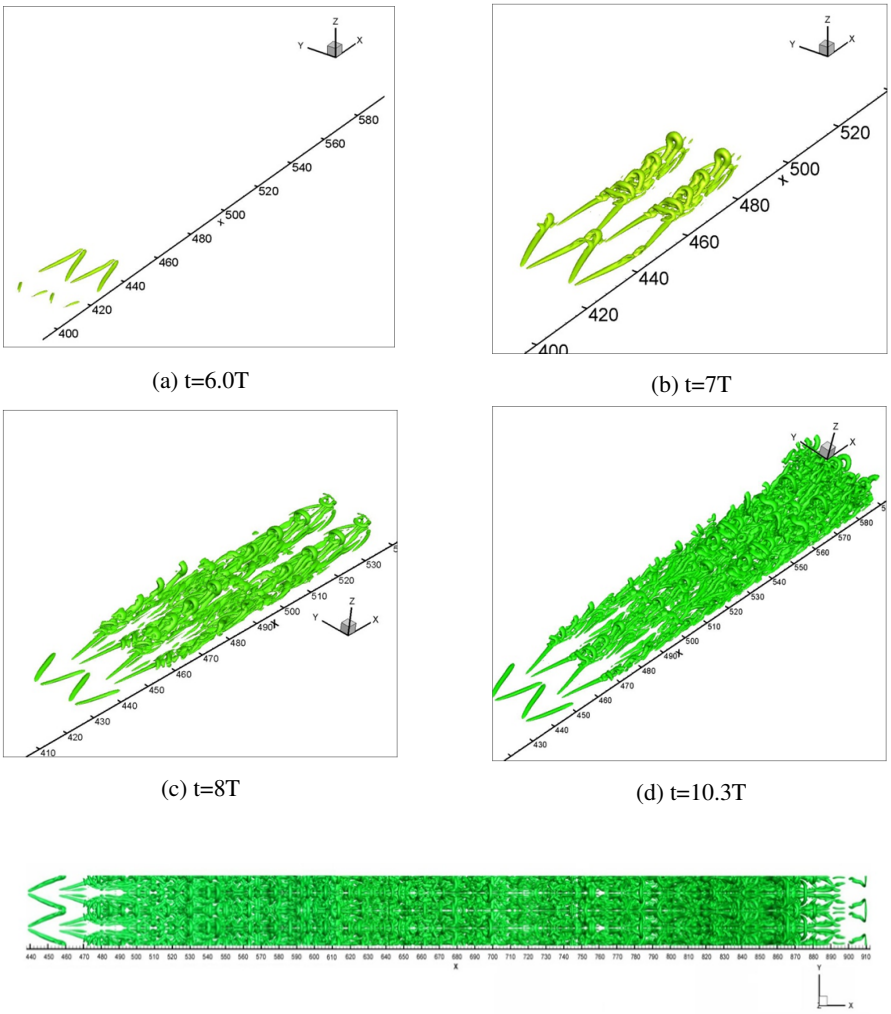

(a) t=6.0T

(b) t=7T

(c) t=8T

(d) t=10.3T

(e) t=17.0T

Figure 10: Evolution of vortex structure at the late-stage of transition(Where T is the period of T-S wave). **(For the purpose of clear visualization, the color of vortex sturucture is changed after t= 8T)**

## 3.2 Chaos of Flow Starts from Second Ring Cycle in Middle

Here we consider the flow field which is viable through our DNS. Figure 11 (a) and (b) are top and bottom view of vortices structure at t=16.25T. We can clearly see from the figure 11(a) that the top ring structures are symmetric.

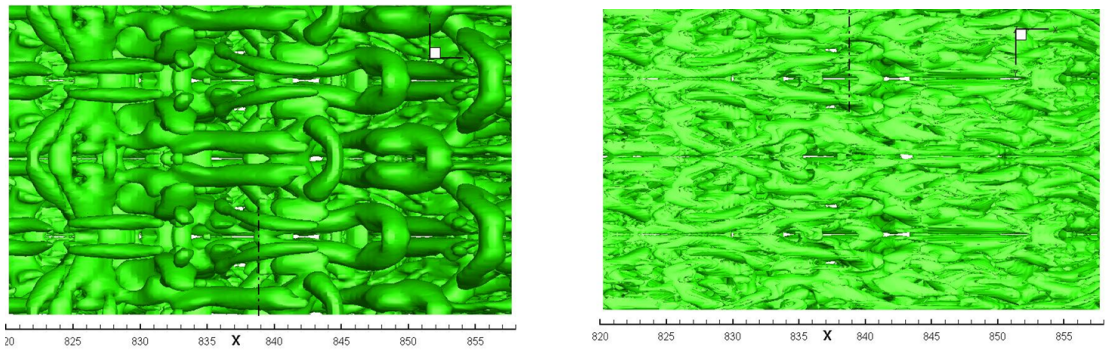

(a) Top view

(b) Bottom view

Figure 11: Asymmetric phenomenon started in middle while top and bottom still preserve symmetry(t=16.75T).

To investigate the symmetriness of the bottom structure, a slice in streamwise direction of flow field has inserted at very bottom. From figure 12(a) and 12(b) it seems that the bottom structure is still symmetric.

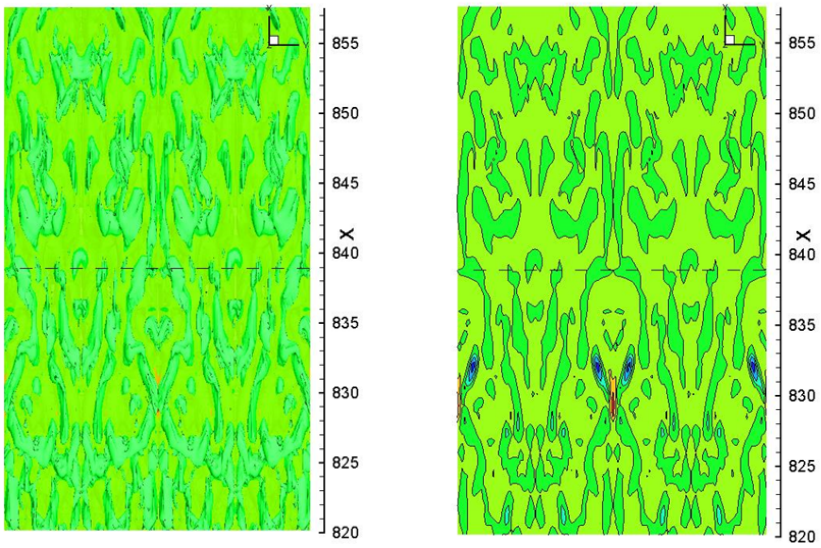


(a) Bottom view with a slice

(b) Bottom Slice with flood and line

Figure 12: Bottom ring cycle structure (t=16.75T).

Meanwhile,to investigate the mechanism of flow chaos in spanwise direction, a slice from Figure 11(a) is chosen in stremwise direction at x=838.9$\delta_{in}$. With the development of advanced tools and technologies in our morden era of research, we found Streamtraces are useful to check intensity of vortices.We can clearly see from Figure 13(a) that the two vortex rings inside left and right white rectangular boxes are generated with different intensity of verticity.Figure 13(b) is the enlarged cross section of 13(b). However, all other vortices have same magnitude of intensity.

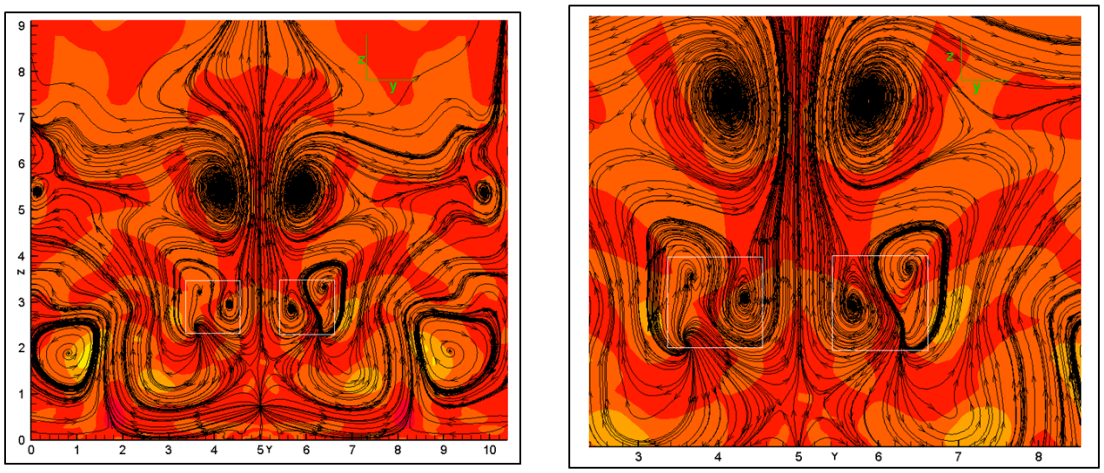


(a) Cross- section of $\lambda_2$ and streamtrace

(b) Enlarged cross-section of $\lambda_2$ and streamtrace

Figure 13: Asymmetric phenomenon started in middle while top and bottom still preserve symmetry(t=16.75T).

To justify that the two vortices indeed have different intensities, we further check two other variables namely pressure and spanwise vorticity ($\Omega_y$). From Figure 14(a), we see that there is less pressure at the left vortex ring position in black rectangle than in the right black rectangle. Also, from Figure 14(b), we can visualize that left vortex ring has greater intensity of spanwise vorticity than the right vortex ring. This observation is consistant with the theory that vortex core always has low pressure.

We further try to confirm our claim ( subsection 3.2) by using 3-dimensional coherent vertical structures. Here, we cut our domain in such a way that the visible tail of vertical structure starts from exactly the same slice in Figure 13 and Figure 14. Figure 15 is tail view of isosurface of $\lambda_2$ at t=16.25T. From the black rectangles in Figure 15, it can be clearly observe that the vortex structures are not symmetric. From here on, we will consider the above mentioned time

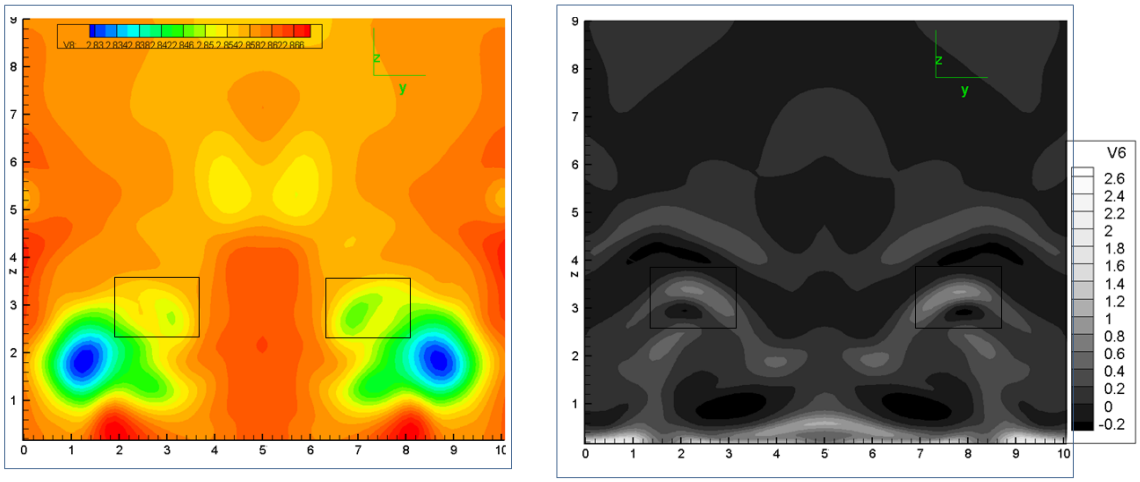


(a) Cross- section of pressure

(b) Cross-section of spanwise vorticity

Figure 14: Asymmetric phenomenon started in middle while top and bottom still preserve symmetry(t=16.75T).

step and streamwise location- t=16.25T,x=838.9$\delta_{in}$ - as the origin of such kind of flow chaos becasue a significant assymetric phonomenon started from that time step and the location. The phonomenon of losing symmetry from the middle ring structure is resonable also. Since each ring cycle itself is very stable structure, it will be symmetric until it start changing position in spanwise direction.The bottom ring cycle structure is in inviscid zone where it get support from the solid wall so it still keeps symmetry. At the same time the top ring cycle is in inviscid region where the flow is regular so the top will remain symmetric until the sweeps push up the assymetric small lenth scales to the top . Hence, the only possibile region for assymetric phenomenon is middle ring cycle structure.

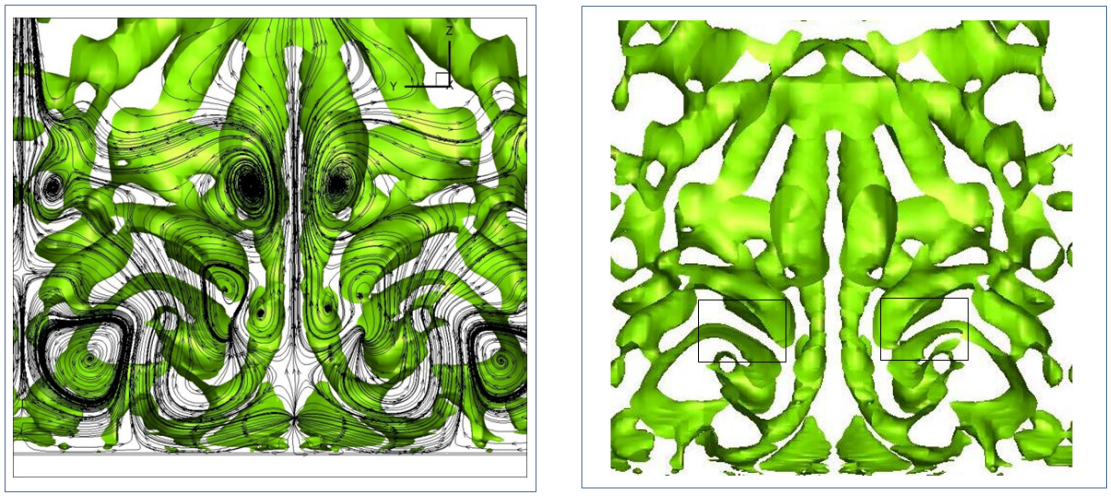

(a) tail view of isosurface of $\lambda_2$ and streamtrace

(b) Enlarged cross-section of tail view of isosurface of $\lambda_2$

Figure 15: Asymmetric phenomenon started in middle while top and bottom still preserve symmetry(t=16.75T).

### 3.3 Overlapping of Multiple Ring Cycles

Figure 16 is a side view of isosurcface of $\lambda_2$ at t=16.25T. From this Figure, we observe that the transitional boundary layer is getting thicker and thicker. This thickening is due to overlapping of multiple ring cycles. This overlapping phenomenon can be described in this way. Since, the ring head is located in the inviscid area and has much higher moving speed than the ring legs which are located near the bottom of the boundary layer, the hairpin vortex is stretched and multiple rings are generated. This will lead to an overlapping of second ring cycle upside of the first ring cycle. However, no mixing of two cycles is observed by our new DNS (Figures 10(c) and 9(d)). The second ring cycle is generated by the wall surface, then separated from wall and convected to downstream. By the same reason the third ring cycle overlaps first two cycles and so on. This is the reason why the transitional boundary layer becomes thicker

and thicker.

While investigating the mechanism for flow chaos, it is found an interesting connection between the origin of chaos (x=838.9$\delta_{in}$) and thickness of transitional boundary layer. From figure 11, it can be observed that the assymetric flow starts from the place where the boundary layer has maximum thickness. More interestingly, it is found that the loss of symmetry happens in the middle of the flow field in the streamwise direction. Since, all noises are mainly introduced through the inflow, outflow or far field, it is unlikely that the reason to cause asymmetry is due to the large background noises, but is pretty much the internal property of the multiple level vortex structure in boundary layers.

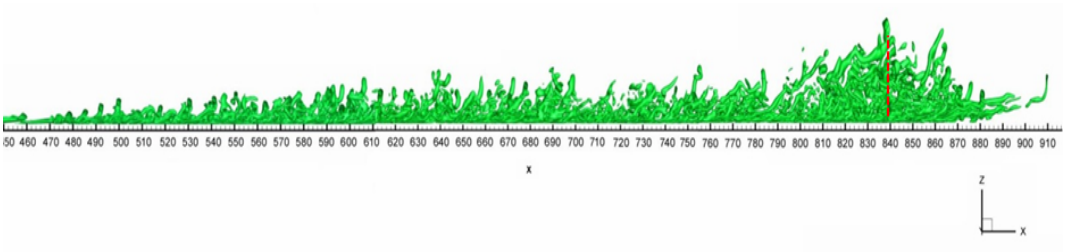


Figure 16: Side view of isosurface of $\lambda_2$ for whole domain

## 3.4 Completely Chaotic Flow at Very Late Stage

As we found the asymmetric fluctuation is originated at the middle level ring cycle. Another question is immediately raised how this loss of symmetry spreads in the normal direction. To answer this question, we investigate the coherent vertical structures at t=17.625T.By observing Figure 17(a), we notice the top level rings still preserve symmetry. Meanwhile we found that the bottom level of ring cycles completely lost symmetry (Figure 17b). This can be concluded that the asymmetric phenomenon which was started in the middle just affected bottom level ring cycle through sweeps. Here we found "Sweeps" motion play important role to spread the asymmetric phenomenon to bottom. Actually, the sweep brings high speed fluid from inviscid region to bottom of boundary layer. The small length scale in bottom is direct consequence of sweeps so these small scales are now victim.

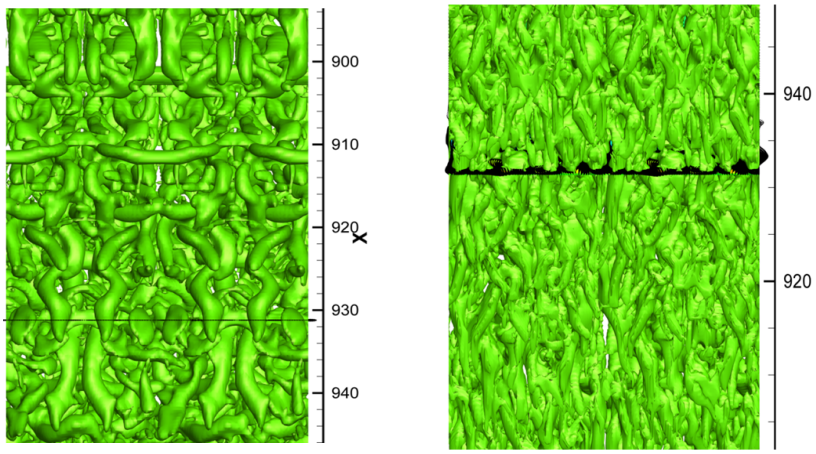


(a) Top view isosurface of $\lambda_2$ (b) Bottom view isosurface of $\lambda_2$

Figure 17: Assymetric phenomenon has spreaded to bottom

To further confirm the claim that the deformed vortices in middle affect the small scale on bottom, we choose a cross section in fig 17 (a) and (b) at $x \approx 931.5$ and draw streamtraces of perturbation velocity along each vortex (Figure 18a). Here, the assymetric fluctation has just spreaded to bottom while top structure is still symmetric. Figure 18(b) is one cross section taken from figure 2o.

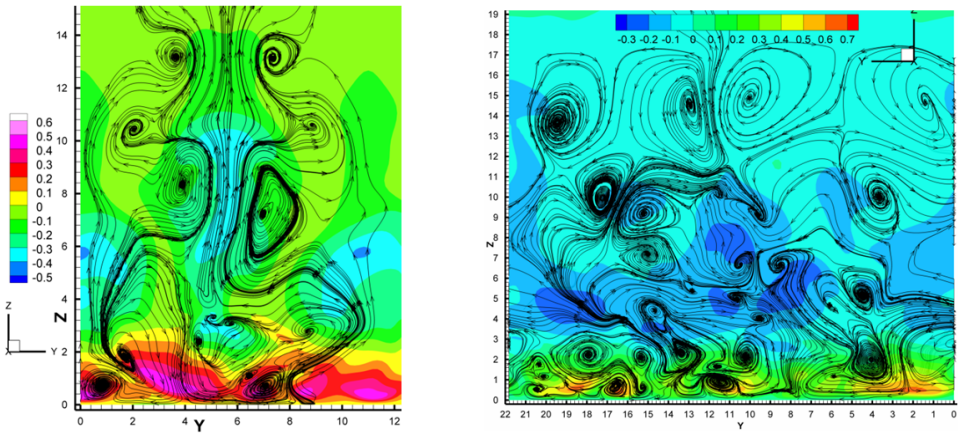

(a) Velocity perturbation

(b) Velocity of streamtracs

Figure 18: Completely assymetric flow at very late stage

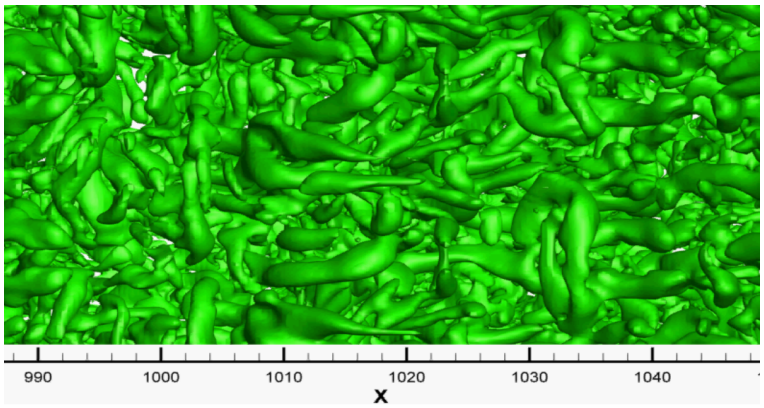


Figure 19: Top view of isosurface of $\lambda_2$

## 4 Hypothesis

Apparently, loss of symmetry, which is equivalent to adding sin(2ky)[3] , is a key issue for the starting point of flow chaos. A hypothesis is given by Liu that the loss of symmetry is caused by the shift from C-type to K-type transitions or reverse. The chaos is caused by the instability of the multiple level vortex ring cycle structure which is an internal property. Therefore, the formation of chaos in late boundary layer transition is not mainly caused by big background noises or removal of periodic boundary conditions in DNS. The flow shows a C-typed transition (staggered) at beginning (Figure 20(a)), but becomes K-type transition later (Figure 20(b)) and then mixed (Figure 20(c)). This means the first vortex circle is C-type, but second circle, which overlaps the first circle, is K-type. K-type, C-type, and mixed type are all observed by experiment. There must be some trend of shift from C-type to K-type or reverse. This shift will cause the loss of symmetry of the middle of the second circle (Figure 21). This trend will change the underneath large ring structure and cause the loss of symmetry of the underneath large rings. Once the middle large rings lost symmetry, the underneath small length scale will lose the symmetry quickly due to the asymmetry of sweeps. Finally, the asymmetry of lower level vortex structures will affect the top rings through ejection and the whole flow field becomes turbulent.

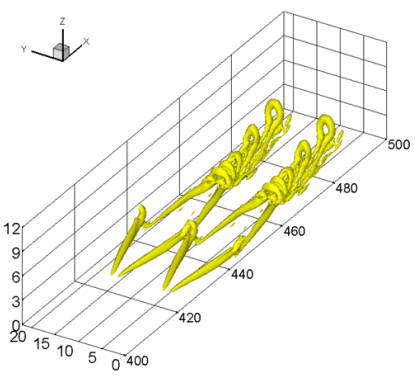


(a) C-type (t=7T)

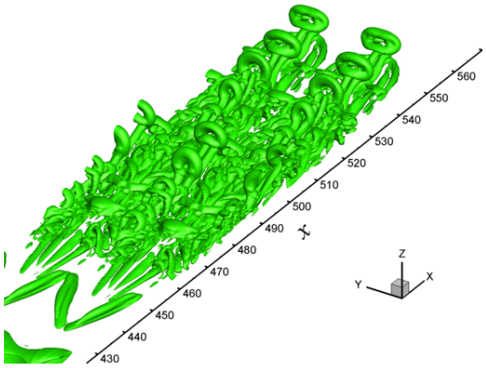


(b) K-type $(t = 10.7T)$

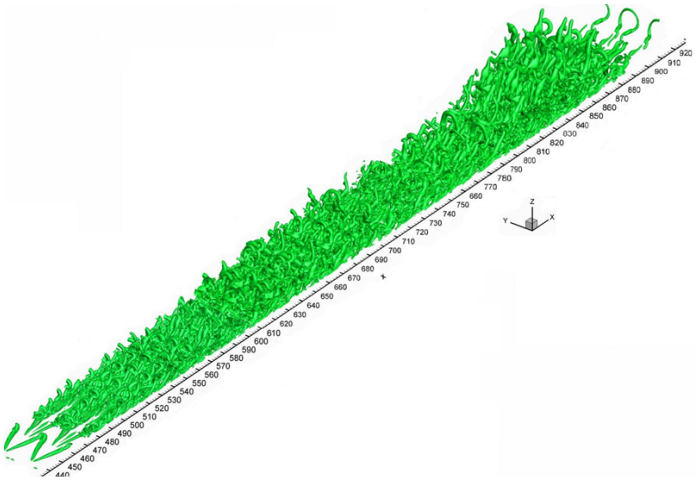

(c) Overlapping multiple ring cycles (t=15.5T)

Figure 20: Vortex structure in K-type, C-type and mixed type transition (T is the T-S period)

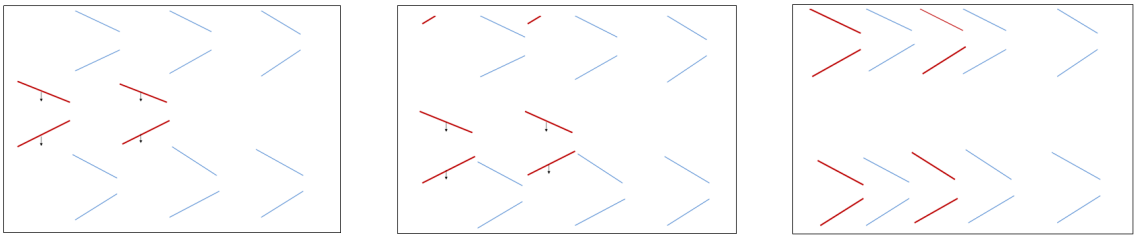

(a) C-type (Symmetric) (b) C-H shift (Non-symmetric) (c) K-type (Symmetric)

Figure 21: Sketch of symmetry loss due to the shift from C-type transition (vortex circles are staggered) to the K-type transition (vortex circles are aligned) (the blue one is the first circle and the red one is the second circle)

## 5 Conclusion

We use the symmetric boundary condition (period is $\pi$ for inflow and $2\pi$ for the whole domain) without any introduction of background noises from the inflow, outflow, and far-field, However, we still find that the assymetric phonomena in middle at first and then in the whole flow field. Following conclusions can be made by from our DNS result:

(a) The noticeable phenomenon of flow chaos is first observed at the second level of the overlapping multiple ring cycles instead of the ring tip. Moreover, the loss of flow symmetry is also found at the middle part of the flow field in the streamwise direction. However, the bottom ring cycle structure still keep symmetric characteristics.

(b) There are small vertex rings generated at the middle by different streamwise velocity shear levels which will affect the intensity of positive spikes. This will result in deformation of the small vortices near the bottom of the boundary layer.

(c) The small background noise due to numerial methods could prompt the C-type to K-type. Eventually, the loss of symmetry may be caused by the shift from C-type to K-type transitions or reverse, and the flow chaos is caused by the instability of the multiple level vortex ring cycle structure which is an internal property.

(d) Finally, the top flow structure also loses the symmetry and the whole flow field assymetric and then chaotic.

## Acknowledgments

This work was supported by The Department of Mathematics at University of Texas at Arlington. The authors are grateful to Texas Advanced Computing Center (TACC) for providing computation hours. This work is accomplished by using Code LESUTA which was released by Dr. Chaoqun Liu at University of Texas at Arlington in 2009.

## REFERENCES

[1] Bake S., Meyer D., Rist U., *Turbulence mechanism in Klebanoff transition:a quantitative comparison of experiment and direct numerial simulation*, J.Fluid Mech, 2002 , 459:217-243.

[2] MEYER D.G.W., RIST U., KLOKER M.J(2003),*Investigation of the flow randomization process in a transitional boundary layer*, In: Krause, E.; Jger, W. (eds.): High Performance Computing in Science and Engineering 03, Transactions of the HLRS 2003, pp. 239-253 (partially coloured), Springer.

[3] Lu P., Thapa M., and Liu C. *Numerical Study on Randomization in Late Boundary Layer Transition*, AIAA 2012, Nashville, TN, January 2012.

[4] Boroduln V. I., Gaponenko V. R., Kachanov Y. S., et al. *Late-stage transition boundary-Layer structure: direct numerical simulation and exerperiment*, Theoret.Comput.Fluid Dynamics, 2002,15:317-337.

[5] Adrian R. J., *Hairpin vortex organization in wall turbulence*, Physics of Fluids, Vol 19, 041301, 2007

[6] Chen L., Tang D., Lu P., Liu C., Evolution of the vortex structures and turbulent spots at the late-stage of transitional boundary layers, Science China, Physics, Mechanics and Astronomy, Vol. 53 No.1: 114, January 2010b,

[7] Chen L., Liu X., Oliveira M., Tang D., Liu C., Vortical Structure, Sweep and Ejection Events in Transitional Boundary Layer, Science China, Series G, Physics, Mechanics, Astronomy, Vol. 39 (10)

[8] Guo Ha, Borodulin V.I., Kachanov Y.s., Pan C, Wang J.J., Lian, X.Q., Wang, S.F., *Nature of sweep and ejection events in transitional and turbulent boundary layers*, J of Turbulence, August, 2010

[9] Jeong J., Hussain F., *On the identification of a vortex*, J. Fluid Mech. 1995, 285:69-94

[10] Duros F., Comte P., Lesieur M., *Large-eddy simulation of transition to turbulence in a boundary layer developing spatially over a flat plate* J.Fluid Mech, 1996, 326:1-36

[11] Jiang L., Chang C. L. (NASA), Choudhari M. (NASA), Liu C., *Cross-Validation of DNS and PSE Results for Instability-Wave Propagation*, AIAA Paper 2003-3555, The 16th AIAA Computational Fluid Dynamics Conference, Orlando, Florida, June 23-26, 2003

[12] Liu X., Chen L., Oliveira M., Tang D., Liu C., *DNS for late stage structure of flow transition on a flat-plate boundary layer*, AIAA Paper 2010-1470, Orlando, FL, January 2010a.

[13] Kachnaov Y. S., 1994, *Physical Mechanisms of Laminar-Boundary-Layer Transition*, Annu. Rev.Fluid Mech., 26, pp. 411482.

[14] Lu P. and Liu C.,*DNS Study on Mechanism of Small Length Scale Generation in Late Boundary Layer Transition*, AIAA Paper 2011-0287 and J. of Physica D, Non-linear, to appear, 2011b, on line: http://www.sciencedirect.com/science/article/pii/S0167278911002612

[15] Rist U. and Kachanov Y.S., 1995, *Numerical and experimental investigation of the K-regime of boundary-layer transition* In: R. Kobayashi (Ed.) Laminar-Turbulent Transition (Berlin: Springer) pp. 405-412.

[16] Wu X. and Moin P., *Direct numerical simulation of turbulence in a nominally zero-pressure gradient flat-plate boundary layer*, JFM, Vol 630, pp5-41, 2009

[17] Chen L and Liu C., *Numerical Study on Mechanisms of Second Sweep and Positive Spikes in Transitional Flow on a Flat Plate*, Journal of Computers and Fluids, Vol 40, p28-41, 2010

[18] Schlichting H. and Gersten K., *Boundary Layer Theory*, Springer, 8th revised edition, 2000

[19] Kolmogorov Andrey Nikolaevich (1941). *The local structure of turbulence in incompressible viscous fluid for very large Reynolds numbers*, Proceedings of the USSR Academy of Sciences 30: 299303. (Russian), translated into English by Kolmogorov, Andrey Nikolaevich (July 8, 1991), *The local structure of turbulence in incompressible viscous fluid for very large Reynolds numbers*, Proceedings of the Royal Society of London, Series A: Mathematical and Physical Sciences 434 (1991): 913. Bibcode 1991RSPSA.434....9K. doi:10.1098/rspa.1991.0075.

[20] Liu C. *Numerical and Theoretical Study on Vortex Breakdown*, International Journal of Computer Mathematics, (to appear)

[21] Kachnaov Y. S., 1994, *Physical Mechanisms of Laminar-Boundary-Layer Transition*, Annu. Rev. Fluid Mech., 26, pp. 411482.

[22] Lu P., Thapa M.and Liu C. *Surface Friction and Boundary Layer Thickening in Transitional Flow*, INTECH (open science/open minds)

[23] Liu C.,Lu P.,Thapa M.,Yan Y. *DNS Study on Turbulence Generation and Sustenance in Late Boundary Layer Transition*, Seventh International Conference on Computational Fulid Dynamics (ICCFD7), Big Island, Hawaii, July 9-13, 2012.